Compartmentalized Phosphodiesterase-2 Activity Blunts β-Adrenergic Cardiac Inotropy via an NO/cGMP-Dependent Pathway

Marco Mongillo, Carlo G. Tocchetti, Anna Terrin, Valentina Lissandron, York-Fong Cheung, Wolfgang R. Dostmann, Tullio Pozzan, David A. Kass, Nazareno Paolocci, Miles D. Houslay, Manuela Zaccolo

Abstract—β-Adrenergic signaling via cAMP generation and PKA activation mediates the positive inotropic effect of catecholamines on heart cells. Given the large diversity of protein kinase A targets within cardiac cells, a precisely regulated and confined activity of such signaling pathway is essential for specificity of response. Phosphodiesterases (PDEs) are the only route for degrading cAMP and are thus poised to regulate intracellular cAMP gradients. Their spatial confinement to discrete compartments and functional coupling to individual receptors provides an efficient way to control local $[cAMP]_i$ in a stimulus-specific manner. By performing real-time imaging of cyclic nucleotides in living ventriculocytes we identify a prominent role of PDE2 in selectively shaping the cAMP response to catecholamines via a pathway involving β_3-adrenergic receptors, NO generation and cGMP production. In cardiac myocytes, PDE2, being tightly coupled to the pool of adenylyl cyclases activated by β-adrenergic receptor stimulation, coordinates cGMP and cAMP signaling in a novel feedback control loop of the β-adrenergic pathway. In this, activation of β_3-adrenergic receptors counteracts cAMP generation obtained via stimulation of β_1/β_2-adrenoceptors. Our study illustrates the key role of compartmentalized PDE2 in the control of catecholamine-generated cAMP and furthers our understanding of localized cAMP signaling. **(*Circ Res*. 2006;98:226-234.)**

Key Words: PDE2 ■ cAMP ■ cardiomyocytes ■ fluorescence resonance energy transfer ■ compartmentalization

The activation of the β-adrenergic system is the primary neurohormonal mechanism controlling force and frequency of cardiac contraction. The majority of β-adrenergic effects are driven by the elevation of intracellular cAMP levels, followed by activation of a cAMP-dependent protein kinase A (PKA). Given the multiple PKA targets within the myocyte, a spatially confined PKA activity is essential to warrant response specificity.[1] It is becoming increasingly evident that the compartmentalization of proteins within specific regions of cardiac myocytes is pivotal to the appropriate functioning of the cAMP/PKA signaling pathway, although the machinery that underpins compartmentalized cAMP signaling is only now becoming fully appreciated.[2] Thus receptors, G_s proteins and adenylyl cyclase (AC) are confined in discrete parts of the plasma membrane,[3] and PKA is anchored via AKAPs (A kinase anchoring proteins)[4] close to its specific targets.[5] cAMP can be compartmentalized in discrete cell regions,[6–8] leading to activation of selected pools of PKA.[8]

Fundamental to the generation and shaping of cAMP gradients is the activity of phosphodiesterases (PDEs),[9] a superfamily of enzymes grouped in 9 families able to hydrolyze cAMP with more than 40 isoenzymes.[9] Instrumental to the generation and shaping of cAMP gradients in cells is the association of PDEs to specific subcellular structures or signaling scaffold complexes via targeting domains.[10] PDE isoenzymes are thus poised to perform unique functional roles that depend on the particular combination of regulatory mechanism, kinetics, and localization.

Members of at least 4 cAMP-PDE families coexist in cardiac myocytes, namely (1) PDE1, a Ca^{2+}/calmodulin activated PDE; (2) PDE2, a cGMP-activated PDE; (3) PDE3, a cGMP-inhibited PDE; and (4) PDE4, a cGMP-independent, cAMP-specific PDE. Of these, PDE3 and PDE4 provide the major PDE activity in the heart,[11] and most studies performed to date have focused on these 2 enzyme families. However, several pieces of evidence suggest that PDE2 may also

Original received November 30, 2004; resubmission received August 2, 2005; revised resubmission received November 22, 2005; accepted December 1, 2005.

From the Dulbecco Telethon Institute (M.M., A.T., V.L., M.Z.) and Venetian Institute of Molecular Medicine (M.M., A.T., V.L., T.P., M.Z.), Padova, Italy; Department of Cardiology (C.G.T., D.A.K., N.P.), Johns Hopkins Medical Institutions, Baltimore, Md; Division of Biochemistry and Molecular Biology (Y.-F.C., M.D.H.), Institute of Biomedical and Life Sciences, University of Glasgow, Scotland, United Kingdom; Department of Pharmacology (W.R.D.), University of Vermont, Burlington; and Department of Biomedical Sciences (T.P.), University of Padova, Italy.

This manuscript was sent to H. Michael Piper, Consulting Editor, for review by expert referees, editorial decision, and final disposition.

Correspondence to Dr Manuela Zaccolo, Venetian Institute for Molecular Medicine, Room G210, Via Orus 2, Padova 35129, Italy. E-mail manuela.zaccolo@unipd.it

Circulation Research **is available at http://circres.ahajournals.org** **DOI: 10.1161/01.RES.0000200178.34179.93**

control important biological functions in heart cells. PDE2 is able to hydrolyze both cAMP and cGMP but is unique in that its N-terminal, paired GAF domains are able to bind cGMP, leading to a concomitant increase in hydrolytic activity.[10] Regarding cardiac function in particular, a cGMP-mediated, PDE2-dependent decrease of cAMP has been reported to be responsible for cholinergic attenuation of β-adrenergic signaling in rabbit atrioventricular nodal cells.[12] Similarly, in pacemaker cells, the effect of NO on heart rate appears to be mediated, at least in part, by inhibition of L-type Ca^{2+} current (I_{Ca}) via a signaling pathway involving guanylyl cyclase activation, synthesis of cGMP, and stimulation of a cGMP-activated PDE.[13] The role of PDE2 in the contractile myocardium is less clear. Although, in amphibian ventricular myocytes[14] and human atrial cells,[15] cGMP has been reported to induce a strong inhibition of cAMP-enhanced I_{Ca} via activation of a cGMP-stimulated PDE, the same effect was not found in other species.[16]

Here we test the novel hypothesis that in cardiac myocytes compartmentalized PDE2 activity blunts β-agonist–induced cardiac contractility via a β_3-receptor–coupled NO-dependent pathway. By using real-time, fluorescence resonance energy transfer (FRET)-based imaging of $[cAMP]_i$ in living cells,[17] we report, for the first time, that consequent to activation of β_3-receptors, there follows a rise in intracellular NO-cGMP levels, which serve to activate membrane-associated PDE2 activity, thereby selectively attenuating spatially confined pools of intracellular cAMP that, ultimately, affect contractile function.

Materials and Methods

Primary cultures of cardiac ventricular myocytes were imaged for FRET changes as described.[8] Confocal immunostaining of PDE2A was performed with a polyclonal antibody (FabGennix). Cell lysis, fractionation method, and PDE assay are described in the expanded Materials and Methods section in the online data supplement available at http://circres.ahajournals.org. Ca_i was assessed by Indo-1 fluorescence, and sarcomere length was measured by real-time Fourier transform (IonOptix MYO100 MyoCam) and whole calcium transient. All methods used in this work are described in detail in the online data supplement.

Results

PDE2 Exerts Tight Control Over cAMP Generated by β-Adrenoceptor Stimulation

We have previously shown that PDE4 and PDE3 families provide the major cAMP PDE activity in rat neonatal ventriculocytes, whereas PDE2 activity is only a minor fraction of the total activity.[11] However, we found that the spatial confinement of specific PDEs can enhance the importance of particular PDE isoforms in determining cAMP signaling.[11] With this in mind, we set out to evaluate the role of PDE2 in the control of cAMP signaling using the specific PDE2 inhibitor erythro-9-(2-hydroxy-3-nonyl) adenine (EHNA) and a genetically encoded, FRET-based sensor for cAMP.[18]

We treated rat neonatal ventriculocytes expressing the genetically encoded cAMP sensor with 10 μmol/L EHNA and found a small increase in $[cAMP]_i$, with a $\Delta/R_0 = 0.9 \pm 0.2\%$ (mean±SEM; n=10) (Figure 1A). Inhibition of all PDE activity with the nonselective inhibitor 3-isobutyl-1-methylxanthine (IBMX) (100 μmol/L), however, generated a rise in $[cAMP]_i$ that was at least ten times larger, with a Δ/R_0 of 10.3±1.5% (n=8) (Figure 1A).

Addition of 10 μmol/L EHNA to ventriculocytes that had previously been stimulated with a submaximal concentration of norepinephrine (NE) (5 nmol/L) resulted in a very large, saturating increase in $[cAMP]_i$ (Figure 1B). The same concentration of NE applied to control cells caused a marginal $[cAMP]_i$ rise. Comparable results were obtained in ventriculocytes from neonatal mice and stimulated with either NE or isoproterenol alone or in combination with EHNA (not shown). To quantify more clearly the effect of PDE2 inhibition in the presence of catecholamines, we used a variant of the cAMP sensor (RII-R230K) showing ≈100-fold higher EC_{50} value in a cAMP-dependent dissociation assay in vitro[11] and found that the response to 1 μmol/L NE showed a 32 $\Delta R/R_0$ of 1.2±1.0% and the subsequent addition of 10 μmol/L EHNA generated a 7-fold increase in $[cAMP]_i$ (32 $\Delta R/R_0 = 6.9 \pm 1.7\%$) (Figure 1C and 1D). Such a response was slightly higher than that recorded with the same sensor after inhibition of total PDE activity with IBMX (100 μmol/L) (Figure 1D).

The low-affinity cAMP probe RII-R230K allows for the investigation of the high range of cAMP concentrations invariably achieved after PDE inhibition. We thus used such a probe in all subsequent experiments, unless otherwise specified. To exclude the possibility that the effect of EHNA on $[cAMP]_i$ was attributable to its known ability to inhibit adenosine deaminase, we challenged cells with NE and EHNA in the presence of the A2a receptor antagonist SCH58261[19] (1 μmol/L). However, this made no difference to the effect of EHNA either in basal or in stimulated conditions (Figure 1E), indicating that EHNA functioned to alter cAMP levels in these cells by inhibiting PDE2 activity.

PDE2 Selectively Controls cAMP Generated by β-Adrenoreceptor Agonists

Although PDE2 represents only a small fraction of total PDE activity in rat neonatal ventriculocytes, the experiments presented in Figure 1 demonstrate that PDE2 inhibition leads to a dramatic augmentation of the β-adrenoreceptor (AR)–induced $[cAMP]_i$. This suggests that PDE2 may be tightly coupled to a pool of AC activated by β-AR. To test this hypothesis, we measured the cAMP response induced by PDE2 inhibition in cells treated with the pharmacological AC activator forskolin. Cells treated with 1 μmol/L forskolin show a rise in $[cAMP]_i$ comparable to that determined by challenge with 1 μmol/L NE ($\Delta R/R_0 = 1.9 \pm 0.1\%$; compare Figures 1B and 2A). Inhibition of PDE2 by EHNA induced an almost undetectable amplification of the cAMP rise in forskolin-treated cells ($\Delta R/R_0$ of 2.2±0.2%) (Figure 2). Thus, the effect of EHNA is more than 30 times larger in the presence of NE than after stimulation with forskolin.

Localization of PDE2

To gain insight into the possibility that PDE2 underpins a compartmentalized effect on cAMP signaling in ventriculocytes, we performed biochemical fractionations of neonatal rat myocytes to determine whether or not PDE2 is membrane

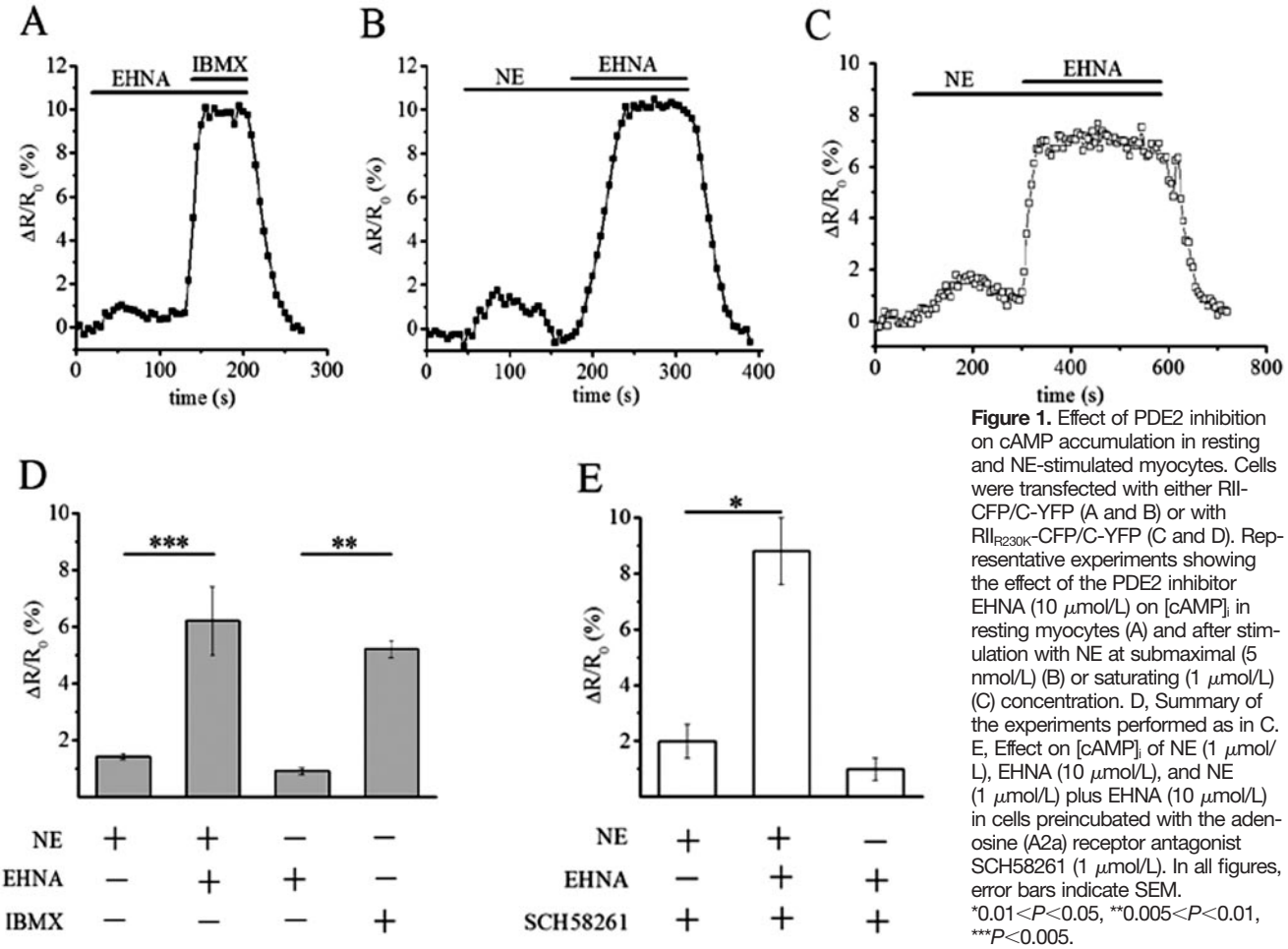

Figure 1. Effect of PDE2 inhibition on cAMP accumulation in resting and NE-stimulated myocytes. Cells were transfected with either RII-CFP/C-YFP (A and B) or with RII_{R230K}-CFP/C-YFP (C and D). Representative experiments showing the effect of the PDE2 inhibitor EHNA (10 μmol/L) on $[cAMP]_i$ in resting myocytes (A) and after stimulation with NE at submaximal (5 nmol/L) (B) or saturating (1 μmol/L) (C) concentration. D, Summary of the experiments performed as in C. E, Effect on $[cAMP]_i$ of NE (1 μmol/L), EHNA (10 μmol/L), and NE (1 μmol/L) plus EHNA (10 μmol/L) in cells preincubated with the adenosine (A2a) receptor antagonist SCH58261 (1 μmol/L). In all figures, error bars indicate SEM. $^*0.01<P<0.05$, $^{**}0.005<P<0.01$, $^{***}P<0.005$.

associated. In doing this, we determined the activity of PDE2, PDE3, and PDE4 in the low-speed (P1) and high-speed (P2) membrane fractions from ventriculocytes as well as in the "soluble" high-speed supernatant fraction (S2). As shown in supplemental Table I, all of the PDE2 activity was recovered in the membrane fraction and no PDE2 activity was detectable in the supernatant. This finding suggests that the PDE2 activity in these cells is entirely attributable to the PDE2A2 isoform, which is membrane associated because of its unique N-terminal extension.[20]

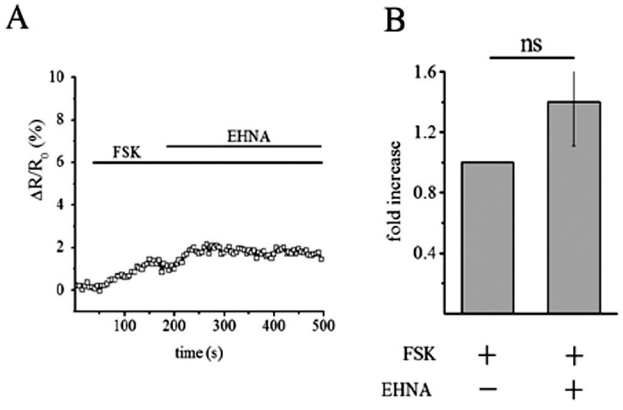

Figure 2. Effect of EHNA (10 μmol/L) on $[cAMP]_i$ generated by 25 μmol/L forskolin (FSK). Representative kinetics (A) and summary (B) of 5 independent experiments. ns indicates not significant.

We further investigated the subcellular localization of PDE2 by immunocytochemistry and confocal microscopy. As shown in Figure 3, PDE2 was found to localize at the plasma membrane and in particular in correspondence of the cell-to-cell junctions. In addition, localization in correspondence of the sarcomeric Z line was clearly detected (Figure 3). A similar localization at the Z line has been shown for PDE4D,[11] an enzyme involved in the selective control of cAMP generated after β-AR stimulation.

Determination of PDE2 Activity in Lysates From Unstimulated and NE-Treated Myocytes

Unlike other PDEs expressed in heart cells (eg, PDE3[21] and PDE4[22]), no stable activation of PDE2 activity has been reported to date. To establish whether our experimental conditions could lead to a stable activation of PDE2 enzymes, we tested PDE2 activity in lysates prepared from both unstimulated and NE-treated cells. The total PDE activity corresponded to 72 ± 6 pmol/min per milligram of protein (mean$\pm$SD, n=5), and the relative PDE2 activity in the same preparations was 2.2 ± 0.8 pmol/min per milligram of protein (n=5). The PDE2 activity in lysates of cells treated, for various lengths of time, with either NE or NE plus EHNA was then determined. The in vitro activity of PDE2 in lysates

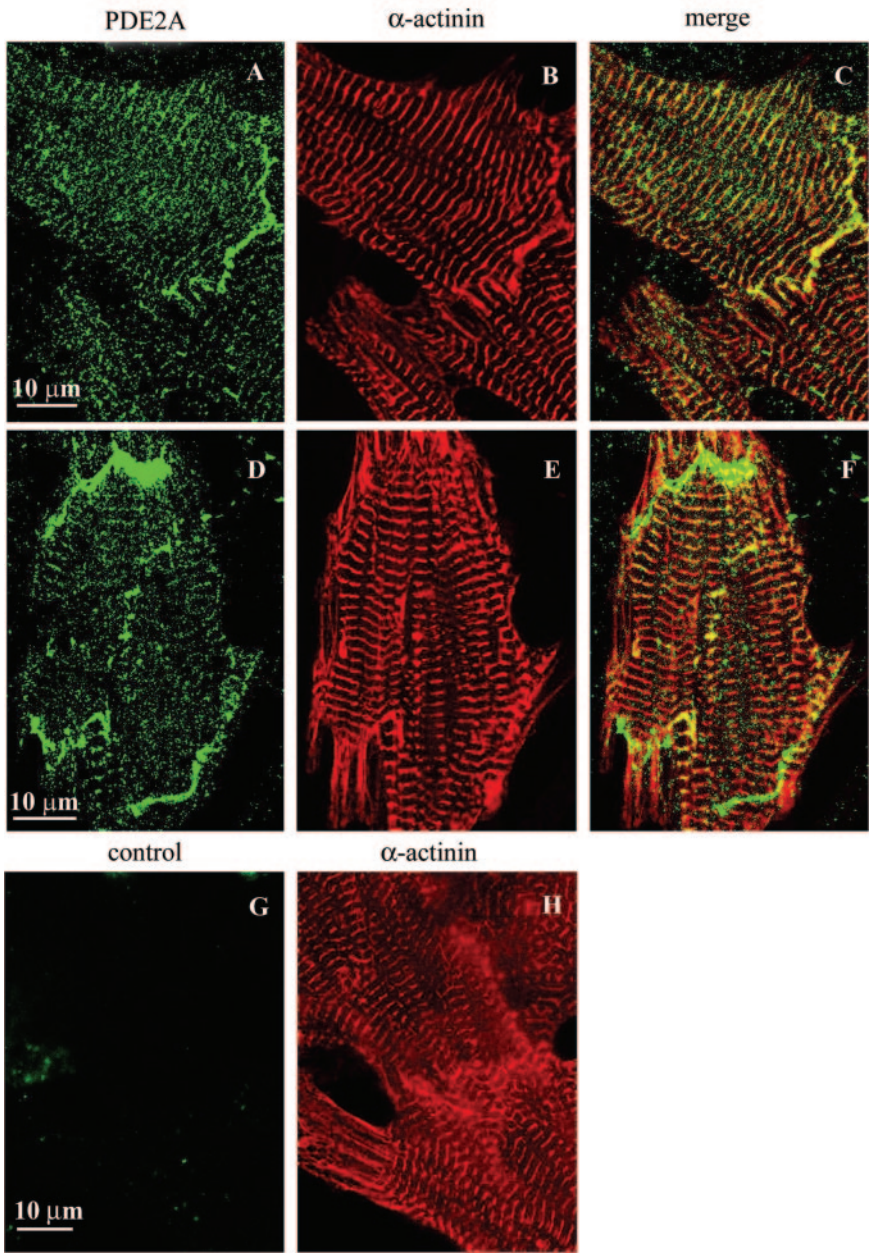

Figure 3. Subcellular localization of PDE2. Confocal images of cultured neonatal rat ventriculocytes supplemented with a polyclonal anti-PDE2 antibody (A and D). As a reference, the immunostaining of the same cells with a monoclonal anti–α-actinin is shown (B and E). C and F, Overlay of the PDE2 and α-actinin staining. Secondary antibody control (G) and α-actinin staining of the same field (H).

treated with 5 nmol/L NE for 1 to 10 minutes and expressed as percent of PDE2 activity at time 0, was 100±7% at 1 minute, 118±11% at 2 minutes, 82±15% at 5 minutes, 122±12% at 8 minutes, and 97±18% at 10 minutes (n=4). Similarly, the effect on PDE2 activity after treatment with 5 nmol/L NE plus 10 μmol/L EHNA was determined as 88±12% at 8 minutes and 91±14% at 14 minutes (n=4). We also tested PDE2 activity on membrane preparations found that the addition of NE had no discernible effect on PDE2 activity (see supplemental Table I). Collectively, these data indicate that no stable increase in PDE2 activity ensued as a result of treating cells with either NE alone or NE together with EHNA.

Indeed, the only known way of markedly potentiating the ability of PDE2 to hydrolyze cAMP is through an increase in cGMP levels.[23] In fact, a 4-fold increase in cAMP-hydrolyzing PDE2 activity has been reported to result from exposure to low micromolar concentrations of cGMP.[24]

NO/cGMP Pathway Modulates the cAMP Response to β-AR Stimulation via PDE2 Activation

To evaluate whether a rise in $[cGMP]_i$ could be responsible for potentiating PDE2 activity after β-AR stimulation, we exploited the fact that the synthesis of cGMP by soluble guanylate cyclases (sGC) is potently activated by NO.

As shown in Figure 4A and 4B, treatment of myocytes with the NO donor sodium nitroprusside (SNP) (10 μmol/L), in the presence of 1 μmol/L NE, reduced the $[cAMP]_i$ rise by ≈50%. SNP, however, had no effect on $[cAMP]_i$ when added to resting cells (not shown). A similar result (reduction of $[cAMP]_i$ of ≈30%) was observed with another NO donor,

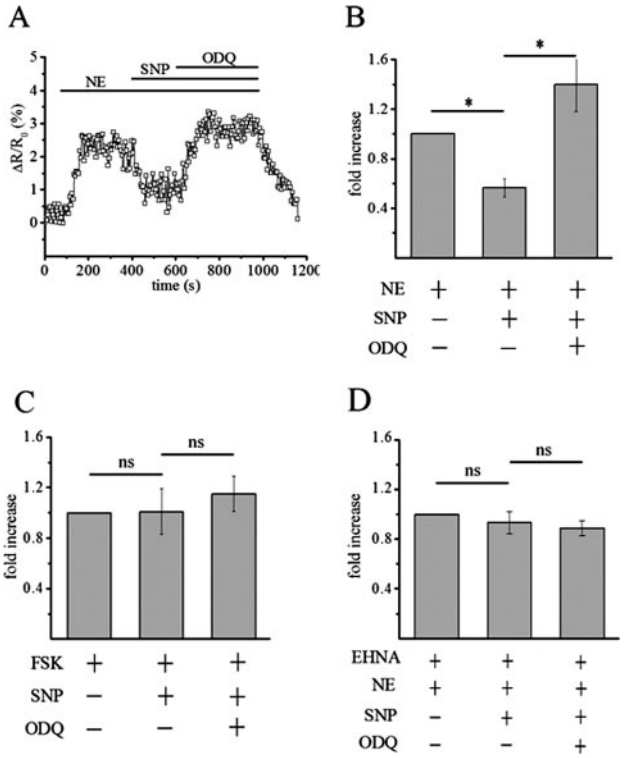

Figure 4. The effect of NO on $[cAMP]_i$ generated by NE. A, Representative kinetic of cAMP changes in cells stimulated with 1 μmol/L NE after addition of the NO donor SNP (10 μmol/L) and the guanylyl cyclase inhibitor ODQ (10 μmol/L). B, Summary of the experiments performed as in A. C, Effect of SNP (10 μmol/L) or ODQ (10 μmol/L) on $[cAMP]_i$ generated by forskolin (1 μmol/L). D, Effect of PDE2 inhibition (EHNA, 10 μmol/L) on cAMP generated by NE (1 μmol/L) in the presence or absence of SNP (10 μmol/L) and ODQ (10 μmol/L). ns indicates not significant.

diethylamine/NO complex (10 μmol/L) (not shown). The reduction of $[cAMP]_i$ induced by SNP was completely reversed and, indeed, was even slightly potentiated by the addition of the sGC inhibitor 1H-[1,2,4]oxadiazolol[4,3,2] quinoxalin-1-one (ODQ) (10 μmol/L[25]) (Figure 4A and 4B). These data indicate that the effect of SNP is mediated by cGMP synthesized by a NO-activated GC. As might be predicted, preincubation of myocytes with ODQ completely prevented the effect of SNP on $[cAMP]_i$ (not shown).

The role of sGC activation in the modulation of NE-generated $[cAMP]_i$ was confirmed by direct activation of sGC using the NO-independent activator BAY41–2272 (10 μmol/L) (not shown).

Interestingly, the effect of NO donors on $[cAMP]_i$ was dependent on the mechanism of the cAMP rise. Indeed, in cells treated with 1 μmol/L forskolin, addition of neither SNP (10 μmol/L) nor ODQ (10 μmol/L) resulted in significant changes in $[cAMP]_i$ concentration (Figure 4C).

The data presented above are compatible with the hypothesis that cGMP modulates β-AR–generated cAMP by increasing PDE2 activity. To confirm this, we measured the effect of SNP and ODQ on NE-generated $[cAMP]_i$ under conditions of PDE2 inhibition. In the presence of 25 μmol/L EHNA, neither SNP nor ODQ elicited any significant change in the $[cAMP]_i$ generated by 1 μmol/L NE (Figure 4 D). When the selective PDE3 inhibitor cilostamide (10 μmol/L) was used in place of EHNA, the effect of SNP and ODQ on NE-generated $[cAMP]_i$ was unchanged (not shown).

NE, via β_3-AR, Counteracts β_1/β_2 Signaling by Increasing Intracellular cGMP

NE activates β_1-, β_2-, and β_3-ARs. Whereas β_1 and β_2 receptors are known to couple to AC to produce cAMP, stimulation of the β_3 receptor isoform leads to the production of NO, which, in turn, stimulates sGC to produce cGMP.[26] To assess whether NE generates a rise of cGMP in cardiac myocytes, we used a genetically encoded, FRET-based probe for cGMP, namely cygnet 2.1′, which allows real-time imaging of cGMP levels in living cells.[27] Transfected ventriculocytes, as expected, responded to SNP with a rapid and dose-dependent increase in $[cGMP]_i$, as detected by a raise in the ratio of 480 nm/535 nm emission after excitation at 430 nm (Δ/R_0) (not shown).

Perfusion with NE (1 μmol/L) of cells transfected with cygnet 2.1 induced a rise in cGMP with a Δ/R_0 of $4.22\pm0.8\%$ ($n=10$) (Figure 5A). This corresponds with $\approx$20% of the maximal effect obtained with 10 μmol/L SNP. An identical effect was observed with a combination of 1 μmol/L NE and the β_1 and β_2 specific antagonists, CGP20712A (300 nmol/L) and ICI118,551 (100 nmol/L), respectively (Figure 5A). Conversely, blockade of the β_3 receptor with the selective

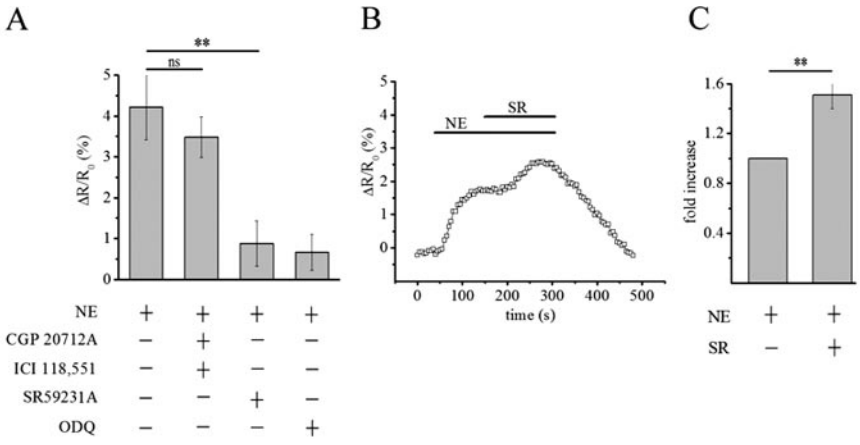

Figure 5. Effect of β_3 AR modulation on cGMP and cAMP levels. A, Generation of cGMP by β-AR stimulation as detected in neonatal rat ventriculocytes expressing the cGMP receptor cygnet 2.1. Selective activation of β_3 receptors was obtained with a combination of NE (1 μmol/L) plus the β_1 antagonist CGP20712A (300 nmol/L) and the β_2 antagonist ICI118,551 (100 nmol/L). Selective blockade of β_3 receptors was attained with the selective β_3 antagonist SR59230A (100 nmol/L). Inhibition of guanylyl cyclase was obtained with ODQ (10 μmol/L). B, Representative kinetics of the cAMP response to NE (10 μmol/L) in the presence of the β_3 selective inhibitor SR59231A (SR) (100 nmol/L). C, Average fold increase of $[cAMP]_i$ in the presence SR59231A (100 nmol/L) over the $[cAMP]_i$ peak amplitude generated by NE. n=5.

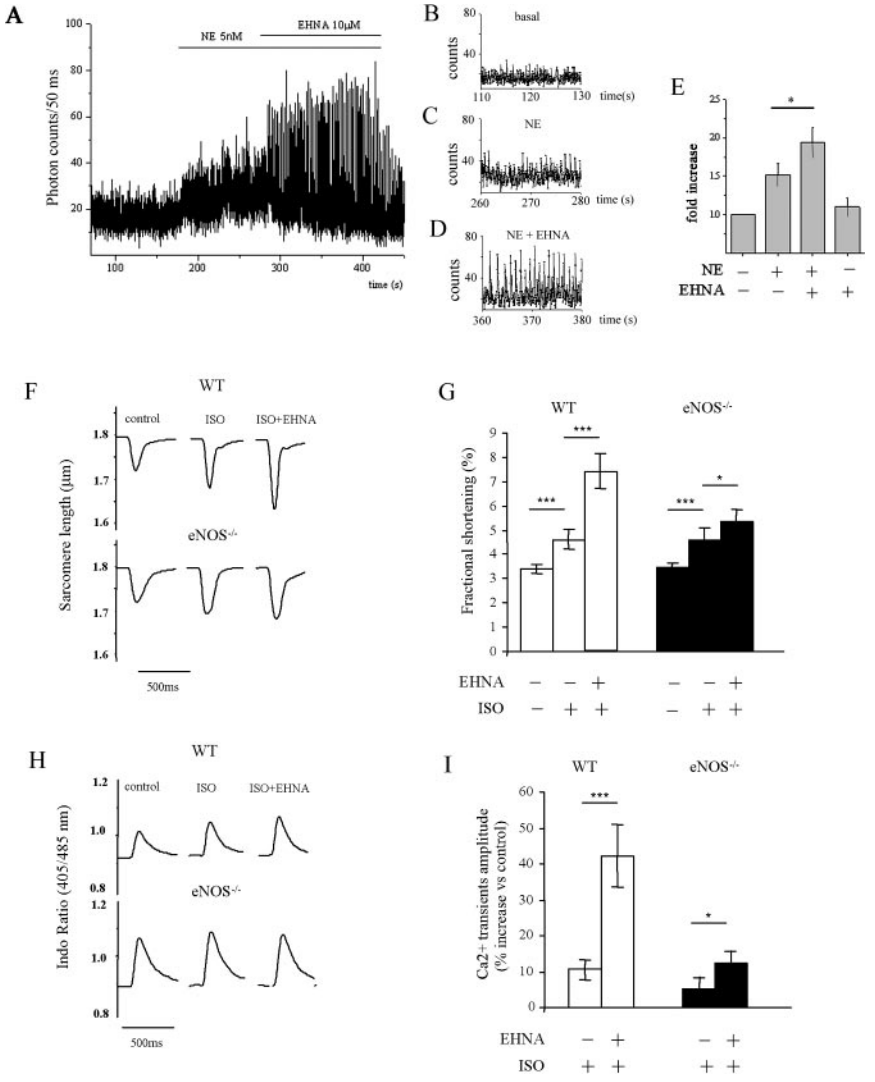

Figure 6. Functional effects of PDE2 inhibition. A, Effect of NE (5 nmol/L) and EHNA (10 μmol/L) on the amplitude (photon counts) of spontaneous cytosolic Ca^{2+} oscillations. B through D, Details of the kinetics shown in A and presented on an expanded time scale. E, Summary of the results of 5 independent experiments performed as in A. Values are expressed as fold increase with respect to the photon counts in non stimulated cells. F, Example tracing showing the fractional shortening recorded in isolated ventriculocytes obtained from adult hearts from wild-type or $eNOS^{-/-}$ mice without any stimulus (control), in the presence of ISO (2.5 nmol/L for WT, or 2 nmol/L for $eNOS^{-/-}$) and the combination of the ISO+EHNA at the same concentrations above. G, Effect of ISO (2.5 nmol/L for WT or 2 nmol/L for $eNOS^{-/-}$) alone or in combination with EHNA (10 μmol/L), on Ca^{2+} transients, as detected by Indo-1 fluorescence changes. The Ca^{2+} transient in the absence of stimulus is also shown (control). H and I, Summary data of the experiments shown in F and G (n=20 for each group).

antagonist SR59230A (10 μmol/L) dramatically reduced the NE effect on $[cGMP]_i$; (Figure 5A). Blockade of cGMP response to NE was also obtained by preincubation of the myocytes with ODQ (10 μmol/L) (Figure 5A).

These experiments indicate the involvement of β_3-AR in the synthesis of cGMP induced by NE and lead to the prediction that β_3-AR stimulation should negatively modulate the cAMP increase triggered by activation of β_1- and β_2-AR. As shown in Figure 5B and 5C, when the β_3-AR was selectively antagonized, NE generated a rise in $[cAMP]_i$ that was ≈1.5 times higher than that in the absence of the β_3-AR antagonist.

β_3-ARs are known to be expressed at very low levels in cardiac myocytes. By performing real-time RT-PCR on neonatal myocytes from rat hearts, we estimated that β_3-ARs represent approximately 0.02% of the total β-ARs (see the online data supplement for details). The very low abundance of β_3-AR in these cells points to a tight coupling between the β_3-AR and its downstream signaling machinery, PDE2, and the pool of β_1/β_2-AR–activated ACs (see also Figure 8).

PDE2 Potently Modulates the Effect of Catecholamine on Intracellular Ca^{2+} Transients and Myocyte Contractility

To evaluate the impact of PDE2 inhibition on ventricular myocyte function, we measured Ca^{2+} transients in spontaneously beating rat neonatal myocytes expressing the genetically encoded Ca^{2+} sensor aequorin.[28] As shown in Figure 6A through 6E, addition of 5 nmol/L NE generated a 1.5-fold increase in the amplitude of Ca^{2+} transients over basal (amplitude of individual peaks averaged over 1 minute interval, $P<0.05$, n=5). A concentration of 10 μmol/L EHNA generated a further significant increase (≈35%, $P<0.05$) of such amplitude, resulting in a 2-fold increase over basal (n=5). We next examined the effect of PDE2 inhibition on myocyte contractility. To this end, we measured sarcomere shortening (SS) in isolated myocytes from adult mouse hearts. In these cells, a submaximal concentration of isoproterenol (ISO) (2.5 nmol/L) increased SS by 34.5±10% ($P<0.005$ versus basal, n=20) and ISO coinfusion with EHNA (10 μmol/L showed a >3-fold increase over ISO [SS: 117±18%, $P<0.0005$

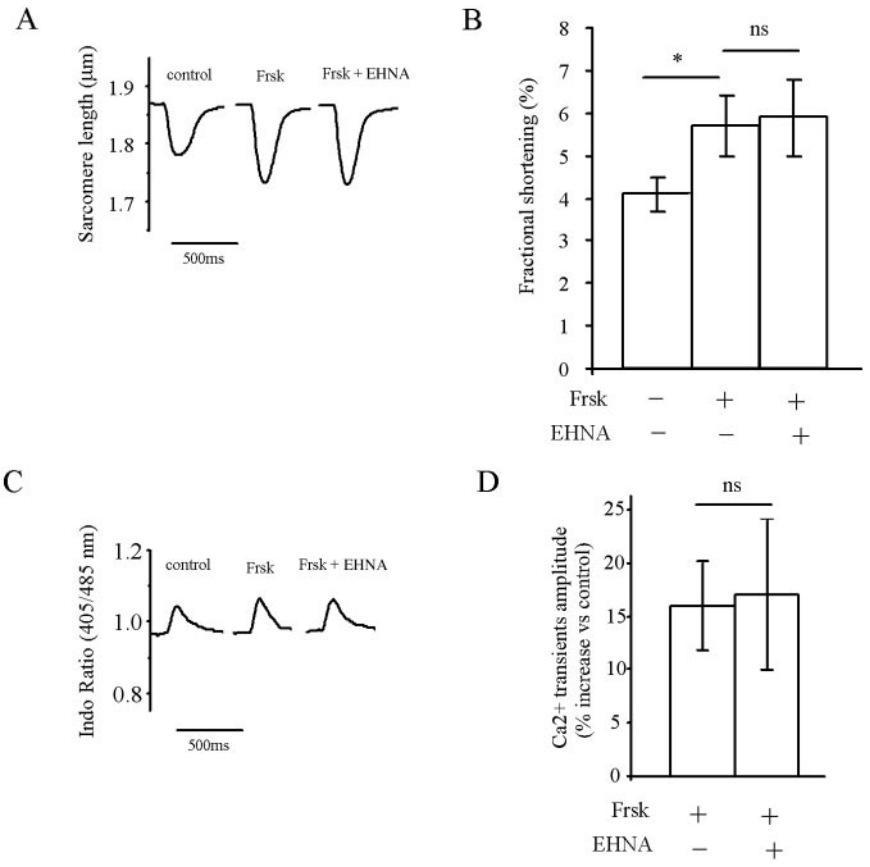

Figure 7. Sarcomere shortening and Ca^{2+} transients amplitudes recorded in isolated adult wt myocytes after stimulation with 10 nmol/L forskolin (Frsk) with or without 10 μmol/L EHNA (example tracings are shown in A and C, respectively, and summary data in B and D, respectively; n=7).

versus ISO alone and $P<0.00005$ versus basal, n=20]; Figure 6F and 6G). Incubation of the cells with ODQ (10 μmol/L) blunted ISO+EHNA–induced SS by more than 50% (41±9% with ISO, $P<0.01$ versus 76±15% with ISO+EHNA, $P<0.01$; all n=16), with a relative increase of ISO+EHNA over ISO of only 84% ($P<0.01$ versus cells not treated with ODQ). Notably, the effect of PDE2 inhibition on contractility was dramatically reduced in myocytes obtained from mice in which the expression of endothelial NO synthase (eNOS) had been abolished by targeted gene ablation ($eNOS^{-/-}$).[29] In $eNOS^{-/-}$ myocytes, we titrated ISO dose (2 nmol/L) to achieve a similar contractility increase as with WT cells. This was done to avoid any possible "saturation" effect, taking into account that $eNOS^{-/-}$ adult murine myocytes show increased cardiac contractile force in response to β-adrenergic stimulation when compared with wild-type (WT) littermates.[30] In presence of 2 nmol/L ISO, SS increase was 32±10% ($P<0.001$ versus basal; P=NS versus ISO in WT cells). In contrast, combining ISO with EHNA led to an additional increase in fractional shortening of only 23% over ISO alone, from 32±10% to 55±17% ($P=0.015$ versus ISO alone, n=20), that was significantly smaller when compared with the same conditions in WT cells ($P<0.01$) (Figure 6F and 6G). The residual effect on fractional shortening after PDE2 inhibition observed in $eNOS^{-/-}$ mice may result from ISO-induced generation of cGMP through an eNOS-independent mechanism. In fact, as shown in Figure 5A, the β_3-AR antagonist SR59230A does not completely abolish NE-induced cGMP, compatible with the existence of a parallel pathway for cGMP generation. In further support of this hypothesis is the observation that in cardiac myocytes cGMP is synthesized in response to ISO even in the presence eNOS inhibitors.[31] The nature of this eNOS-independent pathway to cGMP synthesis remains to be investigated.

The contractility trend was paralleled by consistent changes in Ca^{2+} transients. Basal Ca^{2+} transients were similar between WT and $eNOS^{-/-}$ myocyte groups. ISO stimulation produced an increase in Ca^{2+} transient amplitude of +10.6±3% in WT ($P<0.005$ versus basal) and +5.2±3.3% in $eNOS^{-/-}$ mice ($P=0.05$ versus basal; P=NS versus ISO WT) (Figure 6H and 6I). However, in WT coinfusion of ISO with EHNA increased Ca^{2+} transients by 42.3±8.8% ($P<0.005$ versus ISO alone; $P<0.0005$ versus basal), whereas in $eNOS^{-/-}$ myocytes, this increment was significantly less: +12.4±3% ($P<0.05$ versus ISO/EHNA in WT; $P<0.005$ versus basal; $P<0.05$ versus ISO) (Figure 6H and 6I).

Interestingly, the potentiation effect on SS and Ca^{2+} transient amplitude obtained after PDE2 inhibition in adult myocytes was solely generated in the presence of β-AR stimulation and was not detectable when all AC were stimulated with forskolin (Figure 7), confirming our findings in neonatal myocytes and supporting the tight coupling between PDE2 and the pool of cyclases activated by β-ARs.

Discussion

A large body of evidence indicates that PDEs contribute to the compartmentalization of cAMP signaling.[7,8,10,32] In par-

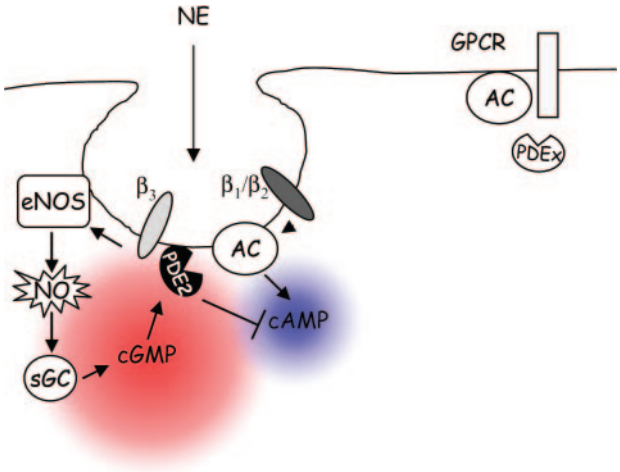

Figure 8. Schematic representation of the proposed β_3-AR feedback control loop. A spatially defined signaling domain includes β-ARs, a selected pool of AC, eNOS, and PDE2. G protein–coupled receptors (GPCR) other then β-AR are localized outside such signaling domain and activate a separate pool of AC. PDE isozymes different from PDE2, and here denoted as PDEx, are responsible for modulating the cAMP response in such separate domains.

ticular, in rat neonatal ventriculocytes, PDE3 and PDE4 show distinct localization[11] and PDE4 appears to be primarily involved in regulating cAMP in a domain harboring the β-AR–activated AC, whereas PDE3 acts in a distinct compartment.[11] In addition, specific targeting of a PDE5A to Z-bands has been reported to selectively enable modulation of ISO-induced contractility in cardiac myocytes.[31] Thus the view is emerging that the functional coupling of distinct PDEs to individual receptors provides an efficient way to control local levels of cAMP in a stimulus-specific manner.[11,17,33]

The present study makes a substantial advancement in our understanding of the role of PDEs in compartmentalized cAMP signaling in that provides evidence that PDE2 plays a key role in the selective control of cAMP generated after β-AR stimulation. Although PDE2 activity provides only ≈3% of total PDE activity in rat neonatal ventriculocytes and PDE2 inhibition showed only a minimal ability to increase $[cAMP]_i$ in unstimulated cells, the contribution of PDE2 was strikingly potentiated in the presence of NE. Such a robust effect of PDE2 on the cAMP response to catecholamines suggests a functional coupling between PDE2 and a pool of AC activated by β-AR stimulation. The finding that PDE2 inhibition has no effect on $[cAMP]_i$ generated through the nonselective activation of all AC with forskolin confirms such a hypothesis.

Targeting of PDE2 to lipid rafts has been reported[34] and, interestingly, β-AR, AC,[3] and NOS[35] are known to reside in the cardiac subtype of lipid rafts known as caveolae. In the present study we found that PDE2 is entirely confined to a membrane compartment, in agreement with the notion that localization of the enzyme to a restricted domain potently enhances its effects on catecholamine-induced cAMP generation. β_3-AR can activate distinct intracellular pathways by coupling to G_s,[36] G_i,[37] and NOS.[26] Although the presence of a β_3-AR/NO/cGMP pathway exerting a feedback control over cAMP has been reported in cardiac myocytes,[26,38] the functional relevance of β_3-AR signaling in the heart is still controversial.[30,39,40] Our data show that β_3-ARs are involved in NE-induced NO generation, leading to sGC activation, synthesis of cGMP, and activation of PDE2. This defines a key role for PDE2 in the attenuation of β-adrenergic signaling via a β_3AR-activated feedback loop (Figure 8).

The functional compartmentalization of PDE2 and β-AR may have important clinical implications. The downregulation of β_1/β_2-AR found in failing cardiac myocytes[41] is accompanied by a significant increase in β_3-AR expression.[42] In addition, β_3-ARs show a relative resistance to homologous desensitization as compared with β_1/β_2-AR.[43] As a consequence, in conditions of high-adrenergic tone, typical of heart failure, β_3-AR–mediated signaling may assume a prominent role and may underlie the progressive nature of functional impairment in heart failure. Interestingly, an increase in PDE2 activity has been recently found in pressure-overloaded ventricles of aortic-banded rats.[44] Thus, in the context of a failing heart, activation of PDE2 via a β_3-AR/NOS/cGMP pathway may further reduce the inotropic reserve and aggravate systolic dysfunction. Selective inhibition of PDE2 may attenuate the negative inotropic effect of β_3-AR signaling and positively influence cardiac performance.

Acknowledgments

This work was supported by Telethon Italy (TCP00089), the Italian Cystic Fibrosis Research Foundation, and the Fondazione Compagnia di San Paolo (to M.Z.); The European Union (QLK3-CT-2002-02149) (to M.Z. and M.D.H.); the Medical Research Council (G8604010) and British Heart Foundation (FS/1999043) (to M.D.H.); Telethon, the Italian Association for Cancer Research, the Italian Ministry of Education, and the Italian Ministry of Health (to T.P.); the National Science Foundation (MCB-9983097) and the Totman Medical Research Trust (to W.R.D.); and the American Heart Association (SDG, 0430144N) and National Institutes of Health (R01 HL075265) (to N.P.).

References

1. Zaccolo M, Magalhaes P, Pozzan T. Compartmentalisation of cAMP and Ca(2+) signals. *Curr Opin Cell Biol*. 2002;14:160–166.
2. Tasken K, Aandahl EM. Localized effects of cAMP mediated by distinct routes of protein kinase A. *Physiol Rev*. 2004;84:137–167.
3. Rybin VO, Xu X, Lisanti MP, Steinberg SF. Differential targeting of beta-adrenergic receptor subtypes and adenylyl cyclase to cardiomyocyte caveolae. A mechanism to functionally regulate the cAMP signaling pathway. *J Biol Chem*. 2000;275:41447–41457.
4. Colledge M, Scott JD. AKAPs: from structure to function. *Trends Cell Biol*. 1999;9:216–221.
5. Kapiloff MS. Contributions of protein kinase A anchoring proteins to compartmentation of cAMP signaling in the heart. *Mol Pharmacol*. 2002; 62:193–199.
6. Buxton IL, Brunton LL. Compartments of cyclic AMP and protein kinase in mammalian cardiomyocytes. *J Biol Chem*. 1983;258:10233–10239.
7. Jurevicius J, Fischmeister R. cAMP compartmentation is responsible for a local activation of cardiac Ca2+ channels by beta-adrenergic agonists. *Proc Natl Acad Sci U S A*. 1996;93:295–299.
8. Zaccolo M, Pozzan T. Discrete microdomains with high concentration of cAMP in stimulated rat neonatal cardiac myocytes. *Science*. 2002;295: 1711–1715.
9. Beavo JA, Brunton LL. Cyclic nucleotide research – still expanding after half a century. *Nat Rev Mol Cell Biol*. 2002;3:710–718.
10. Houslay MD, Milligan G. Tailoring cAMP-signalling responses through isoform multiplicity. *Trends Biochem Sci*. 1997;22:217–224.

11. Mongillo M, McSorley T, Evellin S, Sood A, Lissandron V, Terrin A, Huston E, Hannawacker A, Lohse MJ, Pozzan T, Houslay MD, Zaccolo M. Fluorescence resonance energy transfer-based analysis of cAMP dynamics in live neonatal rat cardiac myocytes reveals distinct functions of compartmentalized phosphodiesterases. *Circ Res*. 2004;95:67–75.
12. Han X, Kobzik L, Balligand JL, Kelly RA, Smith TW. Nitric oxide synthase (NOS3)-mediated cholinergic modulation of Ca2+ current in adult rabbit atrioventricular nodal cells. *Circ Res*. 1996;78:998–1008.
13. Han X, Shimoni Y, Giles WR. A cellular mechanism for nitric oxide-mediated cholinergic control of mammalian heart rate. *J Gen Physiol*. 1995;106:45–65.
14. Mery PF, Pavoine C, Belhassen L, Pecker F, Fischmeister R. Nitric oxide regulates cardiac Ca2+ current. Involvement of cGMP-inhibited and cGMP-stimulated phosphodiesterases through guanylyl cyclase activation. *J Biol Chem*. 1993;268:26286–26295.
15. Rivet-Bastide M, Vandecasteele G, Hatem S, Verde I, Benardeau A, Mercadier JJ, Fischmeister R. cGMP-stimulated cyclic nucleotide phosphodiesterase regulates the basal calcium current in human atrial myocytes. *J Clin Invest*. 1997;99:2710–2718.
16. Mery PF, Lohmann SM, Walter U, Fischmeister R. Ca2+ current is regulated by cyclic GMP-dependent protein kinase in mammalian cardiac myocytes. *Proc Natl Acad Sci U S A*. 1991;88:1197–1201.
17. Zaccolo M. Use of chimeric fluorescent proteins and fluorescence resonance energy transfer to monitor cellular responses. *Circ Res*. 2004;94:866–873.
18. Zaccolo M, De Giorgi F, Cho CY, Feng L, Knapp T, Negulescu PA, Taylor SS, Tsien RY, Pozzan T. A genetically encoded, fluorescent indicator for cyclic AMP in living cells. *Nat Cell Biol*. 2000;2:25–29.
19. Zocchi C, Ongini E, Conti A, Monopoli A, Negretti A, Baraldi PG, Dionisotti S. The non-xanthine heterocyclic compound SCH 58261 is a new potent and selective A2a adenosine receptor antagonist. *J Pharmacol Exp Ther*. 1996;276:398–404.
20. Pyne NJ, Cooper ME, Houslay MD. Identification and characterization of both the cytosolic and particulate forms of cyclic GMP-stimulated cyclic AMP phosphodiesterase from rat liver. *Biochem J*. 1986;234:325–334.
21. Manganiello VC, Degerman E. Cyclic nucleotide phosphodiesterases (PDEs): diverse regulators of cyclic nucleotide signals and inviting molecular targets for novel therapeutic agents. *Thromb Haemost*. 1999;82:407–411.
22. Houslay MD, Adams DR. PDE4 cAMP phosphodiesterases: modular enzymes that orchestrate signalling cross-talk, desensitization and compartmentalization. *Biochem J*. 2003;370:1–18.
23. Martinez SE, Beavo JA, Hol WG. GAF Domains: two-billion-year-old molecular switches that bind cyclic nucleotides. *Mol Interv*. 2002;2:317–323.
24. Michie AM, Lobban M, Muller T, Harnett MM, Houslay MD. Rapid regulation of PDE-2 and PDE-4 cyclic AMP phosphodiesterase activity following ligation of the T cell antigen receptor on thymocytes: analysis using the selective inhibitors erythro-9-(2-hydroxy-3-nonyl)-adenine (EHNA) and rolipram. *Cell Signal*. 1996;8:97–110.
25. Paolocci N, Ekelund UE, Isoda T, Ozaki M, Vandegaer K, Georgakopoulos D, Harrison RW, Kass DA, Hare JM. cGMP-independent inotropic effects of nitric oxide and peroxynitrite donors: potential role for nitrosylation. *Am J Physiol Heart Circ Physiol*. 2000;279:H1982–H1988.
26. Gauthier C, Leblais V, Kobzik L, Trochu JN, Khandoudi N, Bril A, Balligand JL, Le Marec H. The negative inotropic effect of beta3-adrenoceptor stimulation is mediated by activation of a nitric oxide synthase pathway in human ventricle. *J Clin Invest*. 1998;102:1377–1384.
27. Honda A, Adams SR, Sawyer CL, Lev-Ram V, Tsien RY, Dostmann WR. Spatiotemporal dynamics of guanosine 3′,5′-cyclic monophosphate revealed by a genetically encoded, fluorescent indicator. *Proc Natl Acad Sci U S A*. 2001;98:2437–2442.
28. Brini M, Marsault R, Bastianutto C, Alvarez J, Pozzan T, Rizzuto R. Transfected aequorin in the measurement of cytosolic Ca2+ concentration ([Ca2+]c). A critical evaluation. *J Biol Chem*. 1995;270:9896–9903.
29. Shesely EG, Maeda N, Kim HS, Desai KM, Krege JH, Laubach VE, Sherman PA, Sessa WC, Smithies O. Elevated blood pressures in mice lacking endothelial nitric oxide synthase. *Proc Natl Acad Sci U S A*. 1996;93:13176–13181.
30. Godecke A, Heinicke T, Kamkin A, Kiseleva I, Strasser RH, Decking UK, Stumpe T, Isenberg G, Schrader J. Inotropic response to beta-adrenergic receptor stimulation and anti-adrenergic effect of ACh in endothelial NO synthase-deficient mouse hearts. *J Physiol*. 2001;532:195–204.
31. Takimoto E, Champion HC, Belardi D, Moslehi J, Mongillo M, Mergia E, Montrose DC, Isoda T, Aufiero K, Zaccolo M, Dostmann WR, Smith CJ, Kass DA. cGMP catabolism by phosphodiesterase 5A regulates cardiac adrenergic stimulation by NOS3-dependent mechanism. *Circ Res*. 2005;96:100–109.
32. Rochais F, Vandecasteele G, Lefebvre F, Lugnier C, Lum H, Mazet JL, Cooper DM, Fischmeister R. Negative feedback exerted by PKA and cAMP phosphodiesterase on subsarcolemmal cAMP signals in intact cardiac myocytes. An in vivo study using adenovirus-mediated expression of CNG channels. *J Biol Chem*. 2004;279:52095–52105.
33. Baillie GS, Sood A, McPhee I, Gall I, Perry SJ, Lefkowitz RJ, Houslay MD. beta-Arrestin-mediated PDE4 cAMP phosphodiesterase recruitment regulates beta-adrenoceptor switching from Gs to Gi. *Proc Natl Acad Sci U S A*. 2003;100:940–945.
34. Noyama K, Maekawa S. Localization of cyclic nucleotide phosphodiesterase 2 in the brain-derived Triton-insoluble low-density fraction (raft). *Neurosci Res*. 2003;45:141–148.
35. Ostrom RS, Bundey RA, Insel PA. Nitric oxide inhibition of adenylyl cyclase type 6 activity is dependent upon lipid rafts and caveolin signaling complexes. *J Biol Chem*. 2004;279:19846–19853.
36. Kohout TA, Takaoka H, McDonald PH, Perry SJ, Mao L, Lefkowitz RJ, Rockman HA. Augmentation of cardiac contractility mediated by the human beta(3)-adrenergic receptor overexpressed in the hearts of transgenic mice. *Circulation*. 2001;104:2485–2491.
37. Soeder KJ, Snedden SK, Cao W, Della Rocca GJ, Daniel KW, Luttrell LM, Collins S. The beta3-adrenergic receptor activates mitogen-activated protein kinase in adipocytes through a Gi-dependent mechanism. *J Biol Chem*. 1999;274:12017–12022.
38. Barouch LA, Harrison RW, Skaf MW, Rosas GO, Cappola TP, Kobeissi ZA, Hobai IA, Lemmon CA, Burnett AL, O'Rourke B, Rodriguez ER, Huang PL, Lima JA, Berkowitz DE, Hare JM. Nitric oxide regulates the heart by spatial confinement of nitric oxide synthase isoforms. *Nature*. 2002;416:337–339.
39. Vandecasteele G, Eschenhagen T, Scholz H, Stein B, Verde I, Fischmeister R. Muscarinic and beta-adrenergic regulation of heart rate, force of contraction and calcium current is preserved in mice lacking endothelial nitric oxide synthase. *Nat Med*. 1999;5:331–334.
40. Heubach JF, Rau T, Eschenhagen T, Ravens U, Kaumann AJ. Physiological antagonism between ventricular beta 1-adrenoceptors and alpha 1-adrenoceptors but no evidence for beta 2- and beta 3-adrenoceptor function in murine heart. *Br J Pharmacol*. 2002;136:217–229.
41. Brodde OE. Beta-adrenoceptors in cardiac disease. *Pharmacol Ther*. 1993;60:405–430.
42. Moniotte S, Kobzik L, Feron O, Trochu JN, Gauthier C, Balligand JL. Upregulation of beta(3)-adrenoceptors and altered contractile response to inotropic amines in human failing myocardium. *Circulation*. 2001;103:1649–1655.
43. Thomas RF, Holt BD, Schwinn DA, Liggett SB. Long-term agonist exposure induces upregulation of beta 3-adrenergic receptor expression via multiple cAMP response elements. *Proc Natl Acad Sci U S A*. 1992;89:4490–4494.
44. Yanaka N, Kurosawa Y, Minami K, Kawai E, Omori K. cGMP-phosphodiesterase activity is upregulated in response to pressure overload of rat ventricles. *Biosci Biotechnol Biochem*. 2003;67:973–979.

Circulation Research
JOURNAL OF THE AMERICAN HEART ASSOCIATION

Compartmentalized Phosphodiesterase-2 Activity Blunts β-Adrenergic Cardiac Inotropy via an NO/cGMP-Dependent Pathway

Marco Mongillo, Carlo G. Tocchetti, Anna Terrin, Valentina Lissandron, York-Fong Cheung, Wolfgang R. Dostmann, Tullio Pozzan, David A. Kass, Nazareno Paolocci, Miles D. Houslay and Manuela Zaccolo

Circ Res. 2006;98:226-234; originally published online December 15, 2005;
doi: 10.1161/01.RES.0000200178.34179.93
Circulation Research is published by the American Heart Association, 7272 Greenville Avenue, Dallas, TX 75231

Print ISSN: 0009-7330. Online ISSN: 1524-4571

Materials and methods

Chemicals and reagents.

All chemicals were analytical grade. Norepinephrine, isoproterenol, isobutyl-methyl-xanthine (IBMX), eritro-hydroxy-nonyl-adenine (EHNA) and cilostamide were obtained from Sigma-Aldrich (MO, USA). ICI 118,551 hydrochloride, CGP 20712A, SR 59230A from Tocris Cookson (Avonmouth, UK), DeaNO from Calbiochem-Merck Biosciences (Darmstadt, Germany). Sodium nitroprusside (SNP), BAY41-2272, 1H-[1,2,4]oxadiazolo-[4,3-a]quinoxalin-1-one (ODQ) were from Alexis Biochemicals (Lausen, Switzerland) and SCH58261 was a kind gift from Prof. PG Baraldi, Univ of Ferrara, Italy.

FRET Imaging.

Primary cultures of cardiac ventricular myocytes from 1-2 days old Sprague Dawley rats or C57BL/6 mice (Charles River Laboratories, Wilmington, MA) were prepared as described[1]. After transfection with C-YFP and RII-CFP[2], cells were imaged on an inverted Olympus IX50 microscope, equipped with a cooled-CCD camera (Sensicam QI, PCO, USA), with a software controlled monochromator (TILL Photonics, GmbH, Germany) and a beam splitter optical device (Microimager, Optical Insight, USA). During the experiments cells were perfused with HEPES buffered Ringer's modified saline (1mmol/L $CaCl_2$), at RT (20-22°C). Images were acquired as described before by using custom-made software and processed using ImageJ (Rasband, W.S., NIH, USA). Fluorescence resonance energy transfer (FRET) changes were measured as changes in the 480nm/535nm fluorescence emission intensities upon excitation at 430nm and expressed as the percent 480nm/535nm emission increase over the 480nm/535nm value at time 0s ($\Delta R/R_0$). Statistic significance was determined using the paired Student's *t* test and values of $p< 0.05$ were considered significant.

Immunostaining and confocal imaging.

Cells were co-stained with anti PDE2A polyclonal antibody (FabGennix, Texas, USA) and anti alpha actinin antibodies (Sigma). Alexa fluor 488-conjugated anti mouse antibody and Alexa fluor 543-conjugated anti-goat antibody (Molecular Probes, Oregon USA) were used as secondary antibodies. Confocal images were acquired with a Bio-Rad 2100MP confocal system.

Aequorin measurements

For calcium measurements, myocytes were plated at confluency to obtain a uniformely beating syncytium and transfected with the cyt-Aeq construct[3]. Transfection was performed by using the FuGene reagent (Roche) as previously described[4]. With such method we generally obtain an efficiency of transfection of about 10%. Reconstitution of the functional aequorin was carried out in a modified Krebs–Ringer buffer (125 mM NaCl, 5 mM KCl, 1 mM Na_3PO_4, 1 mM $MgSO_4$, 5.5 mM glucose and 20 mM HEPES pH 7.4) in the presence of 100 μM EGTA supplemented with 1% serum and 5 μM coelenterazine for 1 h at 37°C. After reconstitution , the cells were placed in a perfused, thermostated chamber in Krebs-Ringer buffer supplemented with 1 mM $CaCl_2$. The photons emitted by the sample were collected every 50 ms with an amplified photomultiplier connected to a computer for data storage and analysis (for other details see ref[3]).

Isolation of adult mouse ventricular myocytes

Wild type 2-4 month old mice were anesthetized with intraperitoneal pentobarbital sodium (100 mg/kg/ip). The heart was quickly removed from the chest and aorta retrograde perfused at constant pressure (100 cm H_2O) at 37^{o}C for ~3 min with a Ca^{2+}-free bicarbonate-based isolation buffer containing (in mM) 120 NaCl, 5.4 KCl, 1.2 NaH_2PO_4, 20 $NaHCO_3$, 1.6 $MgCl_2$; and glucose (1 mg/ml), 2,3-butanedione monoxime (BDM, 1 mg/ml),and taurine (0.628 mg/ml), gassed with 95% O_2-5% CO_2. To reduce bacterial or viral contamination, the perfusion setup was washed with 70% alcohol and then rinsed three times with sterilized distilled water before cannulation. The enzymatic digestion was initiated by adding 0.9 mg/ml collagenase type 2 (Worthington Biochemical Co., 299 U/mg) and 0.05 mg/ml protease type XIV (Sigma Chemical Co.) to the

perfusion solution. About five minutes later, the left ventricle was removed, cut into several chunks in the same enzyme solution. This solution containing dispersed myocytes was filtered through a 150 μm mesh and gently centrifuged at 500 rpm for 30 seconds. The cell pellet was then promptly re-suspended in isolation buffer added with 125 μM Ca^{2+} and bovine serum albumin (5 mg/ml). After myocyte separation by gravity (~10 min), the supernatant was aspirated and myocytes resuspended in Tyrode's solution (in mM: 140 NaCl, 10 HEPES, 1 $MgCl_2$, 5 KCl; and glucose, 1 mg/ml) added with 250 μM Ca^{2+}. The final cell pellet was suspended in 1.8 mM Ca^{2+}. All solutions were adjusted to pH 7.45 with NaOH.

Simultaneous measurements of contraction and Indo1 fluorescence

Changes in the Ca_i was assessed by Indo 1 fluorescence. Myocytes were loaded with the membrane-permeable acetoxymethyl ester of Indo 1 (Indo 1-AM), using a 12-min incubation with 100 ul of 1 mM Indo-1 AM prepared with 50% Pluronics (Molecular Probes) and 50% DMSO, at room temperature. A final rinse at room temperature in normal Tyrode solution (30 min) allowed intracellular dye de-esterification. Cells were imaged using field stimulation (Warner instruments) in an inverted fluorescence microscope (Diaphot 200; Nikon, Inc). Sarcomere length was measured by real-time Fourier transform (IonOptix MyoCam, CCCD100M), and whole calcium transient by xenon excitation of Indo-1 fluorescence, as previously reported[5;6]. Myocytes were chosen for study according to previously established criteria[7], i.e. a rod-shaped appearance with clear striations and no membrane blebs, a negative staircase of twitch performance on stimulation from rest, and the absence of spontaneous contractions. The cells were superinfused with Tyrodes solution, and the test solutions were applied with a rapid switcher. Experiments were performed in a dark room, since whole calcium transient was measured by xenon excitation of Indo-1 fluorescence.

At the start of each experiment, cells were field stimulated continuously for 10-15 minutes to establish contractile stability. Recording of twitch amplitude was started during the stabilization period and cell shortening data were collected throughout the whole experiment. When the cells

reached a stable baseline contraction, Ca^{2+} transients was recorded for 30 seconds. Steady-state twitches and Ca^{2+} transients were averaged over 30 s periods. Cell twitch amplitude was expressed as a percentage of resting cell length. Twitch kinetics were quantified by measuring the time to peak shortening and the time from peak shortening to 50% relaxation. Similar measurements were derived to quantify Ca^{2+} transients kinetics.

Myocyte fractionation and phosphodiesterase assay

Cell lysis and fractionation method is modified from that as described by[8]. Media was removed from gelatin pre-coated 6 well plates containing ventriculocytes at concentration of 1 million cells/well and cells were washed twice with PBS. PBS was removed and to each 6 well plate was added 0.5 ml lysis buffer (20 mM Tris-HCl pH7.4, 1 mM dithiothreitol with a complete EDTA free protease inhibitor cocktail tablet (Roche) added per 50 ml buffer). Lysis buffer was drained off and the ventriculocytes scraped into tube. Ventriculocytes were snap frozen on dry ice and left to thaw on ice. They were then manually disrupted using a dounce homogeniser followed by syringing with a needle several times to ensure that cells were fully lysed as assessed both through trypan blue entry and also by evaluating latent lactate dehydrogenase activity. The lysate was centrifuged at 2000 gav for 10mins at 4^0C to generate a P1 membrane pellet fraction. The resulting supernatant was removed and centrifuged at 75,000 gav for 30mins at 4^0C to generate a a membrane pellet fraction together with a S2 high speed supernatant fraction. 0.5ml lysis buffer was added to this high-speed pellet and the centrifugation step repeated. The resultant washed pellet fraction was resuspended in lysis buffer to yield P2 high-speed pellet fraction.

PDE activity was assayed using a modification of the Thompson and Appleman two-step procedure as described previously[9]. Protein concentration was determined using the Bradford method.

Real-time RT-PCR

Total RNA was isolated from cultured rat neonatal cardiac myocytes, freshly isolated rat adipocytes from epididymal fat pads and, as negative controls, from CHO and HEK293Tcell lines by using the TRIzol reagent (Invitrogen, USA). An aliquot of total RNA (1 μg) was reversed transcribed by 1 μl Superscript II (Invitrogen, USA), 1 μl RNAsin, oligo dT primer (0.5 μg), 10 pmol dNTPs 4 μl 5x first strand buffer, 2 μl of 0.1 mol/l dithiothreitol in a final volume of 20 μl. The oligonucleotides used for the detection of cDNA specific for β1, β2, β3 and HPRT are shown in supplementary table II. Real time PCR assay was carried out with LightCycler (Roche Diagnostics, Germany) using QuantiTect SYBR Green PCR kit (Qiagen, USA). 60 ng of cDNA was added to 10 μl QuantiTect SYBR Green Master mix, 10 pmol of each primer in a total volume of 20 μl in water. Cycling conditions were as follow: 95°C for 15 min followed by 50 cycles of 95°C for 15s, 55°C for 20 s, 72°C for 8 s.

Data were collected from three independent mRNA preparations and in each experiment samples were in duplicates. For each set of primers a standard curve was generated in adipocytes. Standard curves for calibration of data were created using cANA derived from adypocyte tissue (where β1, β2, β3 genes are highly expressed). The relative quantity of each transcript was determined using the comparative Ct method by interpolating the Ct values of the unknown samples to each standard curve. Values were then normalized with respect to HPRT gene. Melting curve analysis was also performed after PCR amplification to confirm that there were no primer dimers in the PCR products. The identity of the PCR products of all genes was verified by DNA sequencing.

The expression values for the β1, β2, β3 genes we found in cardiac myocytes resulted to be 92.13%, 7.85% and 0.02% of the total β-receptor complement in these cells, respectively.

Amplification curves for β1, β2 and β3 in heart cells are shown in supplementary Fig1 A. In the same figure the amplification curve obtained with the corresponding primers in the absence of template is also shown. Amplification curves for HPRT and β3 in CHO and HEK293 cells, as well

as template free controls for the same primers, are shown in supplementary Fig 1B and C respectively.

To confirm that the mRNA levels found for β3-AR in cardiac myocytes were not due to contaminating cells different from cardiac myocytes, the same analysis was performed on plastic-adherent non-myocyte cells obtained after a 1h pre-plating of the heart cell suspension. Such sample is heavily enriched in fibroblasts and endothelial cells and contains only a minor proportion of cardiac myocytes. In this sample the total amount of β-AR resulted to be approximately one-third of the total calculated in cardiac myocytes and the relative values for β1, β2, β3 genes resulted to be 11.31%, 88.67% and 0.02% respectively.

References

1. Dostal DE, Rothblum KN, Conrad KM, Cooper GR, Baker KM. Detection of angiotensin I and II in cultured rat cardiac myocytes and fibroblasts. *Am J Physiol*. 1992;263:C851-63.
2. Zaccolo M, De Giorgi F, Cho CY, Feng L, Knapp T, Negulescu PA, Taylor SS, Tsien RY, Pozzan T. A genetically encoded, fluorescent indicator for cyclic AMP in living cells. *Nat Cell Biol*. 2000;2:25-9.
3. Brini M, Marsault R, Bastianutto C, Alvarez J, Pozzan T, Rizzuto R. Transfected aequorin in the measurement of cytosolic Ca2+ concentration ([Ca2+]c). A critical evaluation. *J Biol Chem*. 1995;270:9896-903.
4. Mongillo M, Terrin A, Evellin S, Lissandron V, Zaccolo M. Study of cyclic adenosine monophosphate microdomains in cells. *Methods Mol Biol*. 2005;307:1-13.
5. Takimoto E, Champion HC, Belardi D, Moslehi J, Mongillo M, Mergia E, Montrose DC, Isoda T, Aufiero K, Zaccolo M, Dostmann WR, Smith CJ, Kass DA. cGMP catabolism by phosphodiesterase 5A regulates cardiac adrenergic stimulation by NOS3-dependent mechanism. *Circ Res*. 2005;96:100-9.
6. Katori T, Hoover DB, Ardell JL, Helm RH, Belardi DF, Tocchetti CG, Forfia PR, Kass DA, Paolocci N. Calcitonin gene-related peptide in vivo positive inotropy is attributable to regional sympatho-stimulation and is blunted in congestive heart failure. *Circ Res*. 2005;96:234-43.
7. Capogrossi MC, Kort AA, Spurgeon HA, Lakatta EG. Single adult rabbit and rat cardiac myocytes retain the Ca2+- and species-dependent systolic and diastolic contractile properties of intact muscle. *J Gen Physiol*. 1986;88:589-613.
8. McPhee I, Pooley L, Lobban M, Bolger G, Houslay MD. Identification, characterization and regional distribution in brain of RPDE-6 (RNPDE4A5), a novel splice variant of the PDE4A cyclic AMP phosphodiesterase family. *Biochem J*. 1995;310 (Pt 3):965-74.
9. Marchmont RJ, Houslay MD. A peripheral and an intrinsic enzyme constitute the cyclic AMP phosphodiesterase activity of rat liver plasma membranes. *Biochem J*. 1980;187:381-92.

Supplemental Table I

PDE	P1	P2	S2
PDE2	4.7 ± 1.1	6.6 ± 0.61	ND
PDE3	8.7 ± 2.4	11.6 ± 1.2	5.2 ± 0.9
PDE4	38.3 ± 3.0	15.5 ± 1.5	29.0 ± 1.4

Legend:

Distribution of PDE sub-family activity in fractionated cardiac myocytes. Activity is expressed as pmol cAMP hydrolysed/min/mg protein. Data represent means ± SDM. n = 3 independent experiments. ND = non detectable.

Supplemental Table I

We tested PDE2 activity on membrane preparations (P1 and P2 fractions) by either adding 100nM or 5μM NE directly to the PDE2 assay or by pre-incubating fractions P1 and P2 membrane fractions from ventriculocytes with either 100nM or with 5μM NE for 5 and 10 min prior to assay for PDE2 activity in the presence of such concentrations of NE. In each instance we found that the addition of NE had no discernible effect on PDE2 activity (< 5% change in PDE2 activity; n=3).

Supplemental Table II Primers used for real time RT-PCR

Genes	Sequence	Predicted size (bp)
β_1	F: 5'CCTGGACCGCTACCTCG 3' R: 5'GTTGTAGCAGCGGCGCG 3'	175
β_2	F: 5'ACCTCCTTCTTGCCTATCCA 3' R: 5'CCATGACCACCAGGGGC 3'	157
β_3	F: 5'GCAGCCCGGACTTTCG 3' R: 5'GCTCACCTTCATAGCC 3'	157[a]
HPRT	F: 5'AGTCCCAGCGTCGTGATTAG 3' R: 5'CCATCTCCTTCATGACATCTCG 3'	160

[a] : the reverse (R) primer was designed in the coding region immediately 3' to intron 1 of the rat β3 gene.

Legend to supplemental Figure 1

RT-PCR amplification curves. Each panel shows curves from three independent mRNA preparations and one curve from a template free sample for the indicated gene. A: amplification curves for β1, β2 and β3 in cardiac myocytes. Template free controls for β1, β2 and β3 primers are shown in violet, grey and pink, respectively. B: amplification curves for HPRT and β3 in CHO cells. Template free controls are shown in turquoise for HPRT and in pink for β3. C: amplification curves for HPRT and β3 in HEK293T cells. Template free controls are shown in turquoise for HPRT and in pink for β3.

Supplementary fig.1